Localization of poly(glycidyl methacrylate) grafted on reduced graphene oxide in poly(lactic acid)/poly(trimethylene terephthalate) blends for composites with enhanced electrical and thermal conductivities

Localization of Poly(glycidyl methacrylate) Grafted on Reduced Graphene Oxide in Poly(lactic acid)/Poly(trimethylene terephthalate) Blends for Composites with Enhanced Electrical and Thermal Conductivities

Katanyu Kultravut, Keiichi Kuboyama,* Vladimir Sedlarik, Miroslav Mrlík, Josef Osička, Petra Dròhsler, and Toshiaki Ougizawa

Katanyu Kultravut — Department of Materials Science and Engineering, Tokyo Institute of Technology, Tokyo 152-8552, Japan; © orcid.org/0000-0003-0442-8939

Vladimir Sedlarik — Centre of Polymer Systems, Tomas Bata University in Zlín, 76001 Zlín, Czech Republic; ® orcid.org/ 0000-0002-7843-0719

Miroslav Mrlík — Centre of Polymer Systems, Tomas Bata University in Zlín, 76001 Zlín, Czech Republic; 0 orcid.org/ 0000-0001-6203-6795

Josef Osička — Centre of Polymer Systems, Tomas Bata University in Zlín, 76001 Zlín, Czech Republic; 0 orcid.org/ 0000-0002-4909-9350

Petra Drohsler — Centre of Polymer Systems, Tomas Bata University in Zlín, 76001 Zlín, Czech Republic; 0 orcid.org/ 0000-0001-8471-0613

Toshiaki Ougizawa — Department of Materials Science and Engineering, Tokyo Institute of Technology, Tokyo 152-8552, Japan; ® orcid.org/0000-0002-7761-6909

Keiichi Kuboyama — Department of Materials Science and Engineering, Tokyo Institute of Technology, Tokyo 152-8552, Japan;orcid.org/0000-0001-8928-2283; Phone: +81-35734-2439; Email: kuboyama@mac.titech.ac.jp

ABSTRACT: Interfacial localization of conductive fillers in a cocontinuous immiscible polymer blend is an efficient way of improving the electrical and thermal conductivities of the composite. Conductive path formation at the interface of a cocontinuous structure is expected to provide high conductivity by a smaller amount of the filler, which can be used for applications as conductive materials. In this study, biobased poly(lactic acid) (PLA) was blended with poly(trimethylene terephthalate) (PTT) to make the cocontinuous immiscible polymer blend. Poly(glycidyl methacrylate) (PGMA) was grafted on reduced graphene oxide (rGO) to make a PGMA-grafted rGO (rGO-PGMA). The epoxy group of GMA on rGO-PGMA reacted with the end groups of both PLA and PTT and localized at the interface between PLA and PTT by a two-step blending procedure to form the conductive path between PLA and PTT. From transmission electron microscopy observation, it was found that rGO-PGMA localized between the interface of PLA and PTT. Both electrical and thermal conductivities of the composite were improved, which was confirmed by the electrical volume resistivity and thermal diflusivity measurements, compared with neat polymers and other blends.

KEYWORDS: poly(lactic acid), graphene, composite, conductive composite, interfacial localization

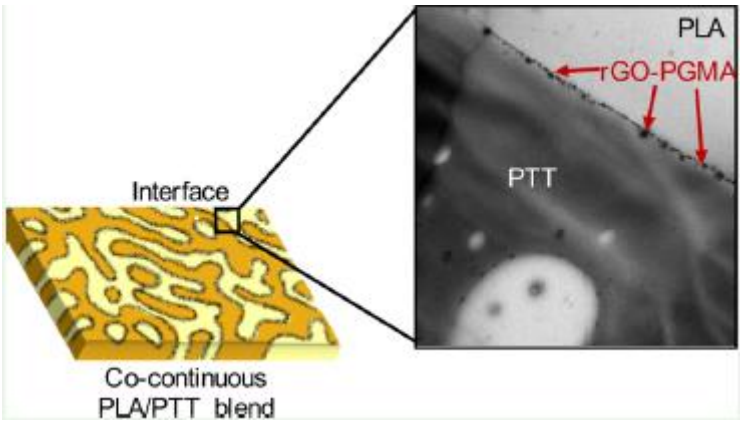

INTRODUCTION

The demand for conductive materials used for electronic devices and other fields has increased in this century. Conductive polymers are paid attention to because of their excellent benefits such as light-weight nature, good processability, and corrosion resistance.[1-3] Many conductive polymers have been synthesized and produced, such as polyacetylene,[4-5] polypyrrole,[6-8] polyphenylene vinylene,[9-10] polyphenylene sulfide,[11,12] and polyaniline.[13,14] However, conductivities and other properties of conductive polymers are not outstanding, and costs are higher compared to commercially conductive materials such as metals. Therefore, synthetic conductive polymer materials are still not being used for commercial conductive applications.[15-17] As conductive polymer materials, conductive polymer composites based on conductive fillers have been used for improving the conductivities of polymers.[18-21] Much attention has been paid to conductive polymer composite because the conductivity of the conductive polymer composite can be controlled in a wide range of conductivity for use in many applications depending on the conductivity such as high conductive applications,[22-24] semiconductors,[25,26] and positive temperature coefficient thermistors.[27,28] Moreover, not only conductive enhancement but also the advantages of polymer matrices including their light weight, high corrosion resistance, and low processing temperature compared with conductive metals are still outstanding after composite preparation. However, as shown in **Scheme 1a**, a high amount of filler loading over the percolation threshold is required to make contact paths of conductive fillers for making conductive materials. The drawback of a high amount of filler loading is not only the reduction of mechanical properties but also the impairing of the molding machine and high cost.[29-32] To reduce the amount of fillers, many researchers have developed techniques for making the conductive path in a conductive polymer composite by using a smaller amount of fillers.

The double percolation technique is one of the methods of filler reduction by localizing the filler only in one phase of a cocontinuous immiscible polymer blend, as shown in **Scheme 1**b. Compared to the composite consisting of a single polymer and the filler, the double percolation technique shows a higher conductivity if the filler fractions are the same.[33-38] Recently, the enhanced development of the double percolation technique, an interfacial localization technique, has gained increasing attention. **Scheme 1**c shows the interfacial localization of the filler at the interface between two phases of the cocontinuous immiscible polymer blend. The conductive paths are successfully achieved with fewer amounts of the filler due to the interfacial localization of the fillers. However, the manufacture of composite construction with interfacial localization of the filler still remains a challenge. Some researchers have investigated the interfacial localization of the conductive filler by many techniques, such as using a kinetics factor or annealing.[39-42] In this study, we tried to use a new technique by using

the chemical modification of the filler surface combining with the blending technique to make the interfacial localization of the filler in a cocontinuous immiscible polymer blend.

Scheme 1. Schematic Representation of Morphologies for the Filler (a) in a Single Polymer Matrix (b) in One of the Polymer Phases of a Cocontinuous Polymer Blend and (c) at the Interface of a Cocontinuous Polymer Blend (Black Dot: Filler, Yellow: Polymer A, and Orange: Polymer B)

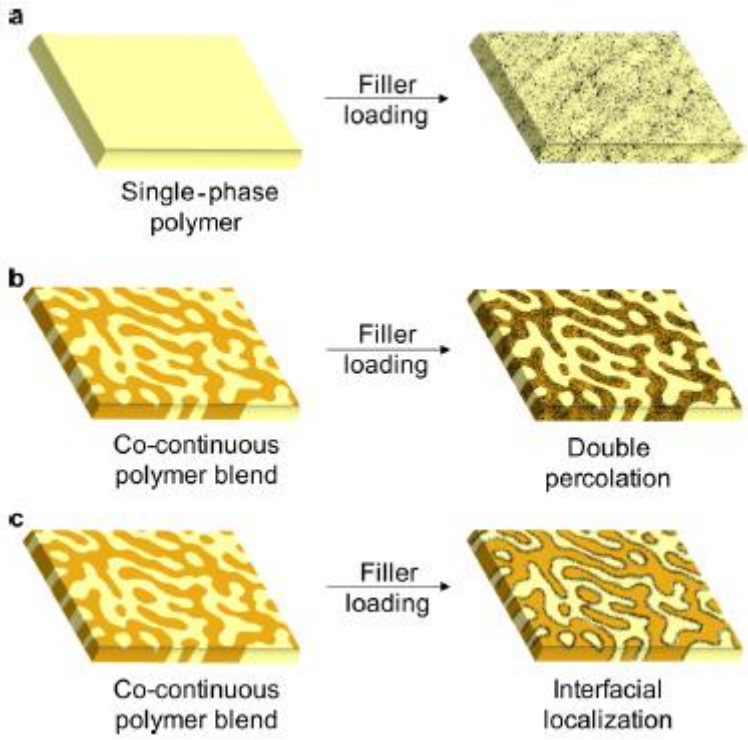

To prepare the interfacial localization of the modified filler in cocontinuous immiscible polymer blend, a blend of biobased poly(lactic acid) (PLA) with a partially biobased aromatic polyester, poly(trimethylene terephthalate) (PTT), was adopted based on our previous studies.[43,44] Previous results have shown that the tensile properties of the PLA/PTT blend have been significantly enhanced by improved interfacial adhesion between PLA and PTT using a reactive compatibil-izer, poly(ethylene-co-glycidyl methacrylate) (PEGMA). The epoxy group of the glycidyl methacrylate (GMA) part in the PEGMA reacted with the end groups of both PLA and PTT, and then, PEGMA was located at the interface between PLA and PTT. Likewise, the concept of the compatibilizer containing the GMA group localizing at the interface between two phases was applied to prepare the interfacial localization of the conductive filler in a cocontinuous polymer blend. In this study, graphene (GE) was chosen as a conductive filler in this research because GE has received great attention owing to its exceptional electrical and thermal properties, which make GE one of the most promising candidates for a filler for high-performance polymer composites.[45-49] Unfortunately, the agglomeration of GE in one of polymer phases is a matter of interfacial localization. Modification of GE with the GMA group was performed for the interfacial localization of **GEScheme 2**. Modification Route of rGO-PGMA between the PLA and PTT in the PLA/PTT blend. The objective of this research has focused on how to localize the modified GE at the interface between PLA and PTT in the PLA/PTT cocontinuous immiscible polymer blend by

the melt blending method to enhance electrical and thermal conductivities of the PLA/PTT/modified GE composite.

Scheme 2. Modification Route of rGO-PGMA

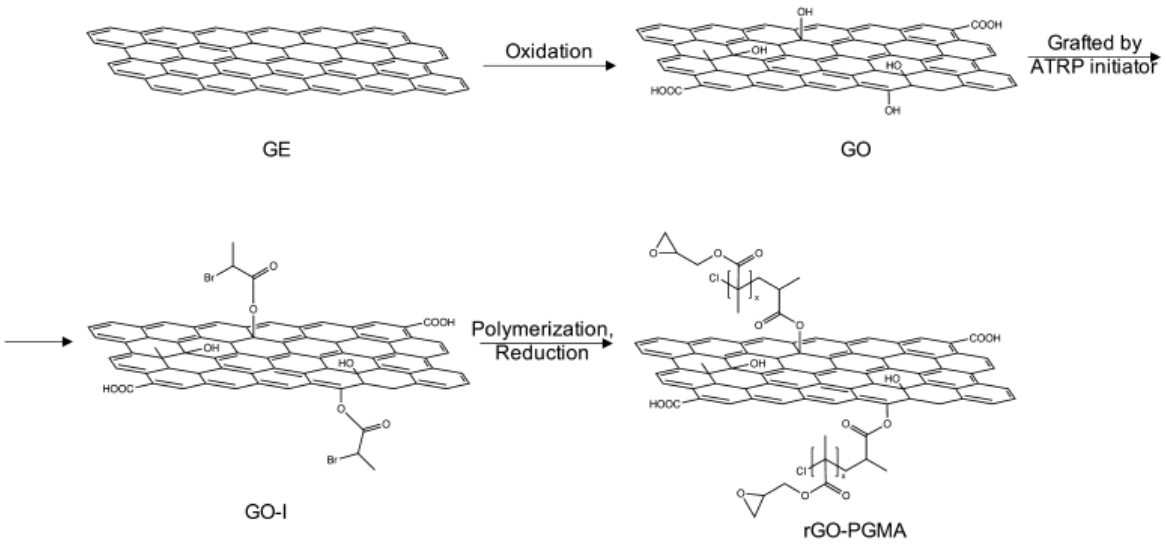

EXPERIMENTAL SECTION

Materials. The high-molecular-weight (M_w) PLA (TP-4000) with the degradation temperature over 300 °C was supplied from Unitika Co., Ltd., Japan, with a L/D content of 98.5/1.5. The PTT pellet (Sorona 3301, NC010) was obtained from DuPont Co., Ltd., Japan, with the M_w of 41,000. GE (ECOPHITG; GFG 50) with a size of 40-55 μm was obtained from SGL Groups Carbon, Germany. All other monomers, reagents, and solvents were purchased from Aldrich and used as received without further purification.

Preparation of rGO-PGMA. To modify GE with the GMA group at the surface, GE was modified by the surface-initiated atom transfer radical polymerization (ATRP) of GMA on the reduced graphene oxide (rGO) method.[50,51] **Scheme 2** shows the modification route of poly(glycidyl methacrylate) (PGMA)-grafted rGO (rGO-PGMA). First, GE was ground and oxidized by the Brodie method to obtain functional groups on the surface to make the graphene oxide (GO).[52] Then, GO was grafted by the ATRP initiator, a-bromoisobutyryl bromide (BiBB), for making an ATRP initiator-grafted GO (GO-I). Finally, polymerization of GMA was performed to make rGO-PGMA. Decreasing content of the hydroxyl groups on the GO surface was achieved by a partial reduction of GO during the ATRP during the polymerization step.

Preparation of PLA/PTT/GE and PLA/PTT/rGO-PGMA Composites. All polymer pellets and fillers were dried in a vacuum oven at room temperature for 48 h before blending to evaporate moisture. To prepare a cocontinuous PLA/PTT immiscible blend, PLA and PTT were mixed together by a melt mixer (Labo Plastomill μ, Toyo Seiki Co. Ltd., Japan) at 240 °C and 120 rpm under N_2 gas for 5 min. The compositions of PLA/PTT blends used in this study were 90/10, 80/ 20, 70/30, 60/40, and 50/50 wt/wt.

For preparation of the composite material, two-step blending was performed on the basis of our previous research.[43] In that study, toughening of PLA by blending with PTT was performed using the reactive compatibilizer of PEGMA. During the melt-mixing process of the PLA/PTT/PEGMA blend, PEGMA preferred to localize in the PLA phase than the PTT one when the three polymers were melt-

mixed simultaneously. To act as a compatibilizer effectively, PEGMA needs to be localized at the interface between PLA and PTT phases. Therefore, the two-step blending was performed according to the following procedure. In the first step, PTT was blended with PEGMA to induce the copolymer formation by the reaction between an epoxy group of GMA and an end group of PTT. Then, PLA was added into the blend in the second step, and the remaining unreacted GMA epoxy group in the PTT-g-PEGMA copolymer reacted with the more favorable PLA during the melt-mixing process at the interface of PLA and PTT phases. As a result, PEGMA which reacted with both PLA and PTT localized at the interface between PLA and PTT and then, it acted as the compatibilizer of the blend. In this study, rGO-GMA was used as a conductive filler instead of PEGMA, which also contains an epoxy group and was expected to react with both PLA and PTT. However, rGO-PGMA also tended to localize in the PLA phase in the PLA/PTT/rGO-PGMA composite similar to PEGMA in the PLA/ PTT/PEGMA blend. Therefore, the two-step blending procedure was also applied in this research as a blending method. That is, PTT was premixed with rGO-PGMA for 2.5 min, then, PLA was added to it, and melt mixing was continued for more 2.5 min (5 min in total as the PLA/PTT blends). As a reference, ground GE was also mixed with the blend by using the same mixing procedure instead of rGO-PGMA. The melt blending conditions of PLA and PTT in the PLA/PTT/GE and PLA/PTT/rGO-PGMA composites were the same as the PLA/ PTT blend. The GE or rGO-PGMA fractions in the polymer composites used in this research were 0.1, 0.2, 0.3, 0.4, 0.5, 0.75, and 1.0 phr. After the melt mixing, all samples were hot-pressed as films with a thickness of around 0.1 mm. After that, all samples were immediately quenched in cold water after the molding to retain the amorphous blend structure.

Fourier Transform Infrared Spectroscopy. The chemical characteristics of the modified GE were investigated by an attenuated total reflection Fourier transform infrared spectroscopy (ATR/FTIR, FT/IR-6800; Jasco Corp., Japan) in the range of 600-4000 cm^{-1} with a resolution of 4 cm^{-1} at room temperature.

Gel Permeation Chromatography. To determine the number-average molecular weight (M_n) of the PGMA chain on the rGO-PGMA, gel permeation chromatography (GPC) (LC-40D prom-inence-i, SHIMADZU, Japan) measurement was performed with the polystyrene standards. Tetrahydrofuran was used as a solvent with a flow rate of 1.0 $mL \cdot min^{-1}$. Anisole was used as an internal standard. Before the measurement, the solutions were filtered (filter hole 0.2 μm). The column was Shodex LF 804, the refractive index detector was RI-71S, and the measurement temperature was 40 °C. The details of the experimental procedure are described in the previous publications.[50,51]

Scanning Electron Microscopy. A fracture surface of the sample was prepared by breaking a sample in liquid N_2. After drying, gold was sputtered on the fracture surface, and the sample was observed by scanning electron microscopy (SEM) (SM-200; Topcon Corp., Japan) under an acceleration voltage of 10 kV at room temperature. Moreover, to confirm the morphology of the blends, only the PLA phase was removed by dissolving in chloroform with a magnetic stirrer for 12 h. After that, the residual samples were washed with distilled water and dried carefully. Finally, morphologies of the blend after removing the PLA phase were observed by the SEM under the same condition described above.

Transmission Electron Microscopy. Locations of GE and rGO-PGMA in the PLA/PTT cocontinuous blends were observed by transmission electron microscopy (TEM) (JEM-1010BS; JEOL Ltd., Japan) under an accelerating voltage of 80 kV. The samples were stained with ruthenium tetroxide vapor before the observation.

Rheological Measurement. A sample for rheological measurement was prepared by compression molding as a disc with diameter 25 mm and thickness 1 mm. The complex viscosity (η*) was measured

with a rheometer (parallel plate, Rheometrics dynamic mechanical spectrometer RDA-II; Rheometrics, Inc., USA) at 240 °C in the frequency range of 0.1-1000 Hz with a constant strain of 3%.

DC Electrical Volume Resistivity. DC electrical volume resistivity measurement (regarded as an inversion of the electrical conductivity) was performed by a picoammeter (Keithley 487, Keithley Instruments, Inc., USA) with a DC voltage source at room temperature. The DC electrical volume resistivity measurement was performed in the thickness direction of the sample with a size of 20 X 20 X 0.1 mm^3. Both surfaces of the sample were coated by silver paste, and copper sheets were attached to each of them. Then, the sample was fixed between two glass slides, and the measurement was performed by connecting the sample to the electrical circuit. Five samples were measured for each filler fraction, and the average value was used.

Thermal Diffusivity. The thermal diffusivity measurement was performed in the thickness direction by an ai-Phase mobile 1u (ai-Phase Co. Ltd., Tokyo, Japan) based on the temperature wave analysis method.[53] The size of the sample was 5.0 X 5.0 X 0.1 mm^3. Thermal diffusivity (α), which is regarded as the ratio of the thermal conductivity of the material to the specific heat capacity of the sample, was calculated using **eq 1**

$$\Delta\theta = -\sqrt{\frac{\omega}{2\alpha}}d - \frac{\pi}{4} \qquad (1)$$

where $\Delta\theta$, ω, and d are the phase delay, angular frequency of temperature wave, and sample thickness, respectively. Five samples were measured for each fraction of the filler, and the average value was used.

Tensile Testing. The sample was molded by compression molding at 240 °C. The gauge length, width, and thickness of the sample were 10, 3, and 0.5 mm, respectively. Tensile testing was performed with a tensile tester (Tensilon UTM-II-20; Orientec Co., Ltd., Japan) at room temperature with a strain rate of 0.167 min^{-1}.

RESULTS AND DISCUSSION

Modification of rGO-PGMA. Figure 1 shows the FTIR spectra of (a) GO, (b) GO-I, and (c) rGO-PGMA, respectively. After oxidization of GE, the peak was observed at 1631 cm^{-1} denoting the stretching vibration of C=O **(Figure 1a)**. The GO exhibited typical absorbing bands of around 3410 cm^{-1} corresponding to the C—O stretching vibrations in C—OH and C—OOH created on the GE surface during the oxidation process. In the GO-I **(Figure 1b)**, the peaks at 1448 and 1370 cm^{-1} assigned to C—O—C stretching vibration corresponding to an initiator and remained functional groups on the GO surface. In the rGO-PGMA **(Figure 1c)**, the peak at 1725 cm^{-1} indicated the C=O stretching vibration, with the peaks at 1460 and 1383 cm^{-1} denoting C—O stretching vibration and the peaks at 1260 cm^{-1} denoting the C—O—C stretching vibration, which comes from the main chain of GMA. The peaks at 930 cm^{-1} represent the epoxy groups from GMA. Successful grafting of PGMA on GO was confirmed from the results. The details of characterization of rGO-GMA can be referred in the previous reports.[50,51]

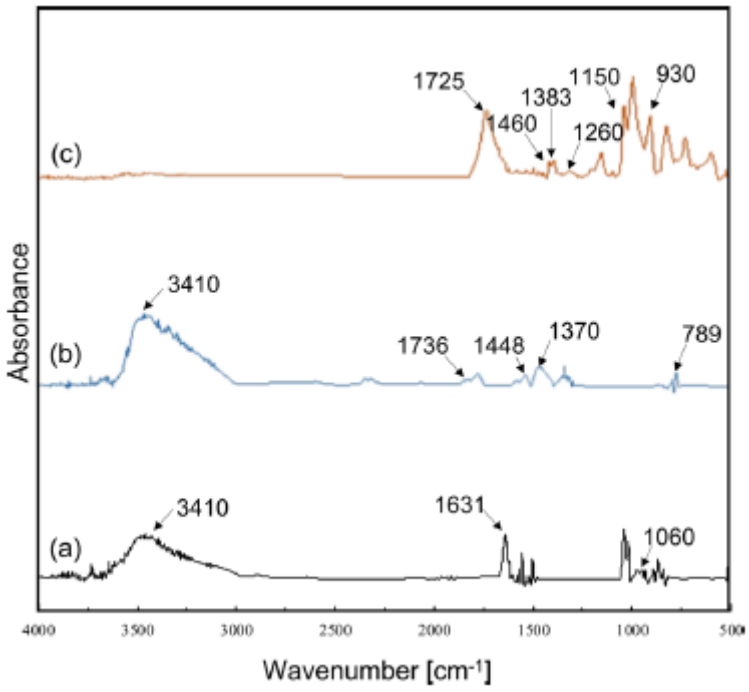

Figure 1. FTIR spectra of (a) GO, (b) GO-I, and (c) rGO-PGMA.

The resistivity of rGO-GMA depends on the M_n of PGMA grafted on rGO.[50] In this study, the M_n of the PGMA on the rGO-GMA was determined by GPC, and the value was 9800 g·mol^{-1}. The DC electrical volume resistivities of the GE and rGO-PGMA were approximately 1.0 X 10^{-6} and 5.0 X 10^{-2} Ω·cm, respectively. Normally, GE has low electrical resistivity (high conductivity) because electrons can move easily in the pi-orbitals. However, the resistivity increased after oxidization to make a GO. Reduction of GO surface groups can cause an enhancement of the conductivity by grafting polymer chain or functional group on the graphene surface affected the resistivity of graphene. From previous research, the different values of M_n of PGMA on the graphene resulted in different resistivities.[50,51] The DC electrical volume resistivities of rGO-PGMA with the M_n of PGMA of 4330, 8500, and 9800 were 8.3 X 10^{-6}, 1.6 X 10^{-6}, and 5.0 X 10^{-2}, respectively.

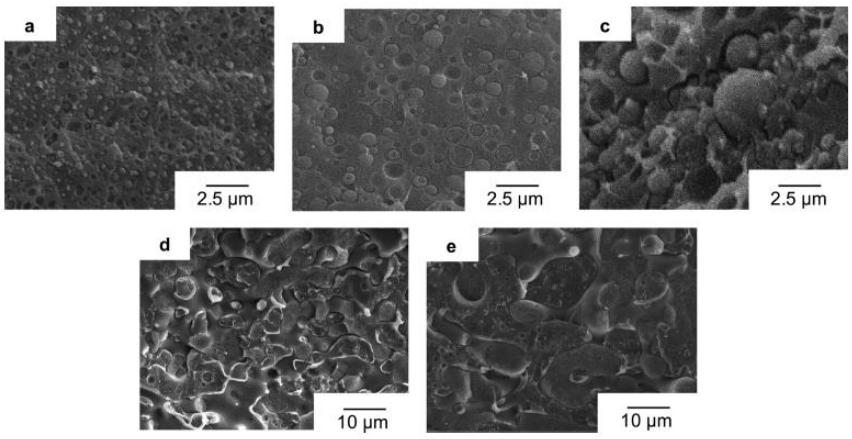

Figure 2. SEM images of fracture surfaces of the PLA/PTT blends in compositions of (a) 90/10, (b) 80/20, (c) 70/30, (d) 60/40, and (e) 50/50 wt/wt.

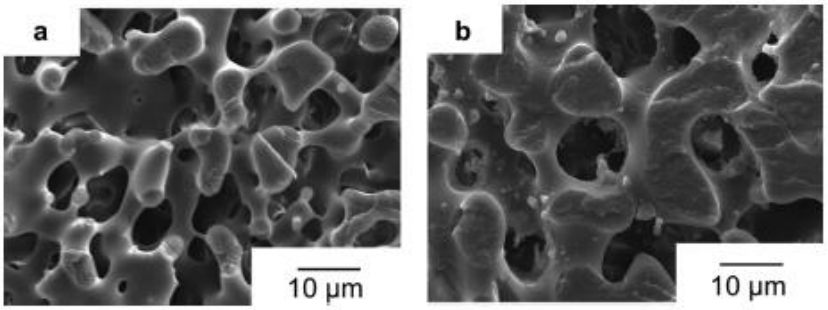

Figure 3. SEM images of fracture surfaces of the PLA/PTT (a) (60/40) and (b) (50/50) blends after removing the PLA phase by chloroform.

After modification, rGO-PGMA shows the higher value of the DC electrical volume resistivity because of the absence of some electron pathways due to the functional groups on the GE surface. Therefore, a smaller M_n of PGMA is desirable for lower resistivity of rGO-GMA, while poor reaction between rGO-GMA and the component polymers in the blend is expected because of smaller amount of the reaction site (GMA). To avoid such a poor reaction, we used this rGO-GMA with a relatively higher molecular weight of PGMA.

Morphologies of PLA/PTT Blends. First, morphologies of the PLA/PTT blends in every composition were investigated to find the blend composition where the cocontinuous structure was obtained. **Figure 2** shows the SEM images of fracture surfaces of the PLA/PTT blends in compositions of (a) 90/10, (b) 80/20, (c) 70/30, (d) 60/40, and (e) 50/50 wt/wt, respectively. A sea-island structure was observed in the PLA/PTT 90/10, 80/20, and 70/30 blends, where PTT particles dispersed in the PLA matrix. Cocontinuous-like morphology was observed in the PLA/PTT 60/40 and 50/50 blends. In order to clarify the blend morphology, only the PLA phase in the blends was removed by solvent etching in order to observe the residual PTT phase, as shown in **Figure 3**a,b, and then, the continuous PTT phase was clearly seen in both PLA/PTT 60/40 and 50/50 blends. The cocontinuous structure of the PLA/PTT 60/40 blend was finer than that of the 50/50 blend. In addition, the sample weight change between the solvent etching before and after was measured to confirm the formation of the cocontinuous structure. Weight losses of the samples by the solvent etching were around 60 wt % in the PLA/PTT 60/40 blend and 50 wt % in the PLA/PTT 50/50 blend. It was confirmed that not only the fracture surface but also the whole sample was cocontinuous. Then, the PLA/PTT 60/40 blend was chosen in this research as a representative to make a conductive composite because the higher content of PLA than PTT was environmentally friendly because PLA is a fully biobased polymer, while PTT is a partially biobased aromatic polyester.

PLA/PTT/GE and PLA/PTT/rGO-PGMA Composites. TEM observation was performed to determine the position of the GE and rGO-PGMA fillers in the composites PLA/ PTT/GE and PLA/PTT/rGO-PGMA. **Figure 4** shows TEM images of (a) PLA/PTT/GE (60/40/0.2) and (b) PLA/PTT/ rGO-PGMA (60/40/0.2) composites, respectively. From **Figure 4**a, the agglomeration of GE (indicated by white arrows) was observed only in the PTT phase (gray region) but not in the PLA phase (white region) or interface between PLA and PTT. This implies that GE did not well disperse in the PLA/PTT blend, and GE preferred to localize only in the PTT phase.

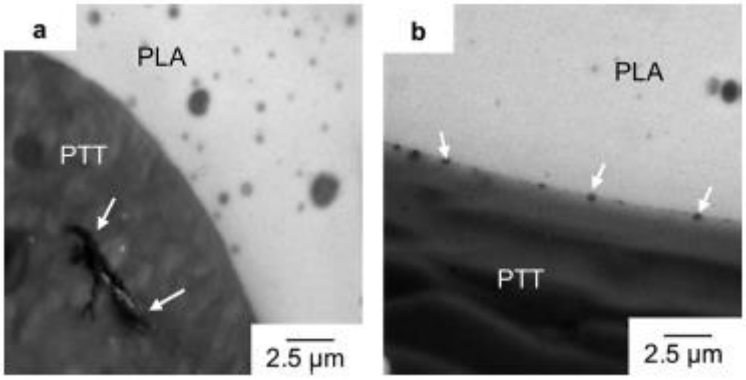

Figure 4. TEM micrographs of (a) PLA/PTT/GE (60/40/0.2) and (b) PLA/PTT/rGO-PGMA (60/40/0.2) composites.

The size of GE was smaller by the sheer force during the composite preparation by the rotating screws of the melt mixer. In the two-step blending procedure, PTT was melt-mixed with GE in the first step, and then, PLA was added to it. The reason why the GE localized only in the PTT phase was because the GE did not react with both PTT and PLA. In contrast, many small rGO-PGMA particles with a diameter of around 0.6 μm (indicated by white arrows) were located at the interface between PLA and PTT, which is shown in **Figure 4**b as a homogeneous structure, and no agglomeration of rGO-PGMA was observed in the composite PLA/PTT/rGO-PGMA. The size of the rGO-PGMA was smaller than the ground GE flake because of the modification process including the grinding and sonication processes. Some rGO-PGMA particles were dispersed in both matrices. However, rGO-PGMA mainly dispersed at the interface between PLA and PTT, which is the main reason of the conductive improvement by using the interfacial localization technique. It was suggested that rGO-PGMA was an effective filler to localize at the interface between PLA and PTT after blending by the two-step blending procedure. From the analogy with the PLA/PTT/ PEGMA blend, it is suggested that the premixing of PTT with rGO-PGMA in the first step of mixing induced the reaction of epoxy group in rGO-PGMA with the functional group of PTT. Subsequently, in the second step, the remaining rGO-PGMA epoxy group continued to react with PLA, and then, rGO-PGMA was located at the interface between the phases of PLA and PTT.

Figure 5 shows the complex viscosity (η*) of the PLA/PTT blend, PLA/PTT/GE composite, and PLA//PTT/rGO-PEGMA composite. The η* of the PLA/PTT/GE composite was higher than that of the PLA/PTT blend. In **Figure 4**a, GE was mainly localized in the PTT domain, and this may have increased the viscosity of the PTT domain and it induced the increase of viscosity of the PLA/PTT/GE blend. Moreover, the η* in the PLA/PTT/rGO-PGMA was highest among the samples. In this composite, rGO-PGMA mainly localized at the interface of the PLA matrix phase and PTT domain. The increase of viscosity implies that the copolymer formation of PLA-g-rGO-PGMA-g-PTT at the interface of the PLA matrix phase and PTT domain takes place, which induces the friction between them.

To investigate the effect of conductive filler location, DC electrical volume resistivity and thermal diffusivity measurements were performed using the thin film samples. The size of the filler after blending in the blend was much smaller than the original size. Therefore, the fillers are not given a structure in the whole composite material. **Table 1** shows the DC electrical volume resistivities and thermal diffusivities of the neat polymers and PLA/PTT (60/40) blend as a reference. **Figure 6**a shows the DC electrical volume resistivities of PLA/PTT/ GE (60/40/x) and PLA/PTT/rGO-PGMA (60/40/x) composites, where x is the weight part of the conductive filler.

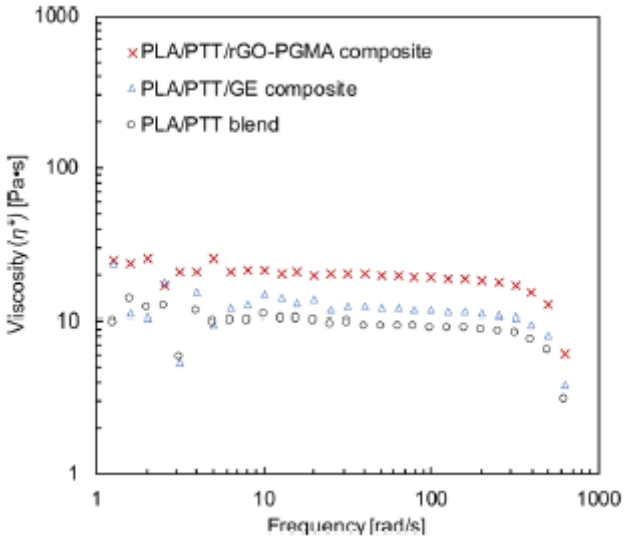

Figure 5. Complex viscosity (η*) of the PLA/PTT (60/40) blend, PLA/PTT/GE (60/40/0.2) composite, and PLA//PTT/rGO-PEGMA (60/40/0.2) composite.

Table 1. DC Electrical Volume Resistivities and Thermal Diffusivities of Neat Polymers and the PLA/PTT Blend

sample	DC electrical volume resistivity [Ω·cm]	thermal diffusivity (α) [10^{-7} m^2 s^{-1}]
neat PLA	3.70×10^{12}	0.74
neat PTT	8.96×10^{11}	0.92
PLA/PTT (60/40) blend	1.62×10^{12}	0.86

The neat PLA, PTT, and PLA/PTT (60/40) blend showed high resistivity as same as a normal polymer, which is an insulating material.[54-56] In the PLA/PTT/GE (60/40/x) composites, the DC electrical volume resistivity was almost the same with the neat PLA/PTT(60/40) blend independent of the filler content. This result indicated that the high conductive GE addition up to 1 phr did not improve the conductivity of the blend. In **Figure 4**a, the agglomeration of GE was located only in the PTT phase, which did not induce connective filler network formation. In contrast, the PLA/PTT/rGO-PGMA (60/40/x) composites showed the lowering of DC electrical volume resistivities by increase of the rGO-PGMA fraction. The resistivity slightly reduced up to 0.3 phr of rGO-PGMA addition to the PLA/PTT blend and was sharply reduced up to around 0.7 phr. The result shows that the percolation threshold of the rGO-PGMA in the PLA/PTT/rGO-PGMA composite, which was determined by the inflection point of the graph, was observed in the range around 0.4-0.5 phr of rGO-PGMA.

Figure 6b shows the thermal diffusivities of the PLA/PTT/ GE (60/40/x) and PLA/PTT/rGO-PGMA (60/40/x) composites. In this plot, the thermal diffusivity of the former was hardly changed regardless of the GE fraction up to 1.0 phr, while the value of the latter was improved depending on the rGO-PGMA fraction up to around 0.7 phr. It was clearly indicated that the PLA/PTT/rGO-PGMA composite's electrical and thermal conductive properties could be enhanced with the small amount of rGO-PGMA less than 0.7 phr.

To confirm conductive filler formation in the PLA/PTT/ rGO-PGMA composite around the percolation threshold, TEM observation of the samples was performed. **Figure 7** shows the TEM micrographs of the PLA/PTT/rGO-PGMA composite with the compositions of (a) 60/40/0.3, (b) 60/ 40/0.4, and (c) 60/40/0.5. It was shown that rGO-PGMA was located at the interface between PLA and PTT in all the samples. The rGO-PGMA particles seem to locate at the interface separately in the PLA/PTT/rGO-PGMA (60/40/ 0.3) composite. In the PLA/PTT/rGO-PGMA (60/40/0.4) composite, some rGO-PGMA made contact with each other, and they almost made contact with each other at 0.5 phr of rGO-PGMA. From the results of TEM micrographs, rGO-PGMA could locate at the interface between the PLA/PTTblend which could be fitted onto the surface of the cocontinuous structure in **Figure 3**. This suggests that the changes in both resistivity and diffusivity of PLA/PTT/rGO-PGMA around 0.5 phr of rGO-PGMA was induced by the formation of a conductive network of rGO-PGMA at the interface of the PLA matrix and PTT domain.

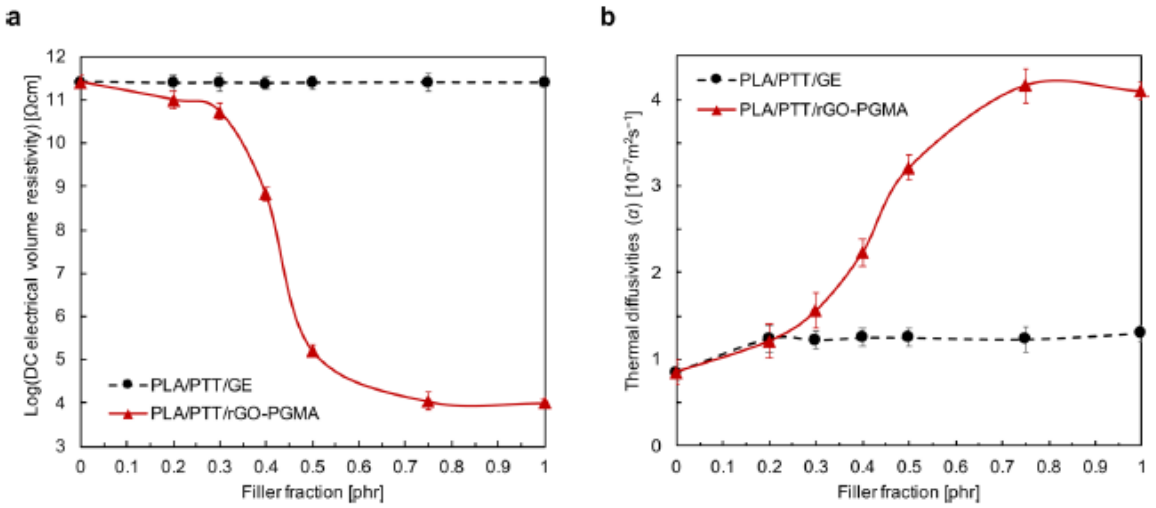

Figure 6. TEM micrographs of the PLA/PTT/rGO-PGMA composite with the composition (a) 60/40/0.3, (b) 60/40/0.4, and (c) 60/40/0.5.

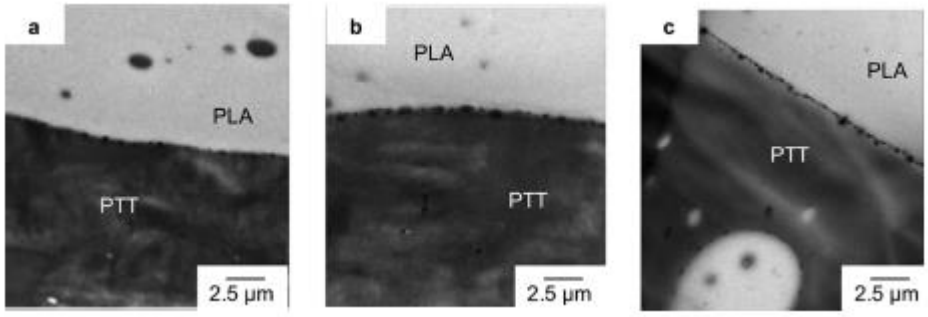

Figure 7. TEM micrographs of the PLA/PTT/rGO-PGMA composite with the composition of (a) 60/40/0.3, (b) 60/40/0.4, and (c) 60/40/0.5.

In this study, we tried to prepare the cocontinuous PLA/ PTT blend with rGO-PGMA localizing at the interface between PLA and PTT phases, and then, the improvement of electrical and thermal conductive properties was investigated. This study achieved the filler fraction less than 0.5 phr to each the percolation threshold with the electrical resistivity around 10^5 Ω·cm, while other studies used 1.0

phr or more with this range of the conductive properties.[41,42] This study demonstrates that modification by the surface-initiated ATRP of GMA on the rGO method combined with the two-step blending procedure could control the localization of the filler at the interface between PLA and PTT. This is a new technique for improving the conductivities of the composite since the former method involved thermodynamic (wetting coefficient) and kinetic (compounding sequence and melt viscosity) factors for making an interfacial localization to make a conductive composite by adding the filler.[57-63] Moreover, tensile properties were analyzed, as shown in **Figure S1**. It was shown that the tensile strength of the PLA/PTT/rGO-PGMA composite was not reduced compared with neat PLA. Moreover, the elongation at break of the PLA/PTT/rGO-PGMA composite was slightly improved to 7.0%. However, the ductile manners were not observed.

CONCLUSIONS

In this study, GE was modified by the surface-initiated ATRP of the GMA method. The PLA/PTT/rGO-PGMA composite was prepared by blending PLA and PTT with rGO-PGMA in a two-step blending process. The effects of conductive fillers were examined. As a result, it was found that using rGO-PGMA as a conductive filler was a successful method to enhance DC electrical volume resistivity and thermal diffusivity of the composite because rGO-PGMA was located at the interface and formed a percolation threshold with low content of the filler. DC electrical volume resistance and thermal diffusivity of the PLA/PTT/rGO-PGMA composite were dramatically increased compared to the PLA/PTT/GE composites in the same filler fraction. Moreover, the percolation threshold of rGO-PGMA in the PLA/PTT/rGO-PGMA composites was investigated. It was shown that low content of rGO-PGMA percolated in the filler content range of 0.4-0.5 phr. Therefore, the PLA/PTT/rGO-PGMA composite produced by the two-step blending shows a high potential for using as conductive application in the future. In this study, both DC electrical volume resistivity and thermal diffusivity saturated above around 0.8 phr of the filler fraction. This result is considered to be because the width of the conductive path is almost same with the diameter of the filler particle as shown in **Figure 7**, which comes from the localization mechanism of the filler, that is, copolymer formation of PLA and PTT through the reactive filler loading. Therefore, both conductivity and thermal diffusivity can be improved by suppression of breakup of the fillers during the sample preparation process.

REFERENCES

(1) Feldman, D. Polymer History. Des. Monomers Polym. 2008, H, 1-15.

(2) Tseng, I.-H.; Chang, J.-C.; Huang, S.-L.; Tsai, M.-H. Enhanced Thermal Conductivity and Dimensional Stability of Flexible Polyimide Nanocomposite Film by Addition of Functionalized Graphene Oxide. Polym. Int. 2013, 62, 827-835.

(3) Supronowicz, P. R.; Ajayan, P. M.; Ullmann, K. R.; Arulanandam, B. P.; Metzger, D. W.; Bizios, R. Novel CurrentConducting Composite Substrates for Exposing Osteoblasts to Alternating Current Stimulation. J. Biomed. Mater. Res. 2002, 59, 499-506.

(4) Saxman, A. M.; Liepins, R.; Aldissi, M. Polyacetylene: Its Synthesis, Doping and Structure. Prog. Polym. Sci. 1985, H, 57-89.

(5) Minto, R. E.; Blacklock, B. J. Biosynthesis and Function of Polyacetylenes and Allied Natural Products. Prog. Lipid Res. 2008, 47, 233-306.

(6) Bolto, B.; McNeill, R.; Weiss, D. Electronic Conduction in Polymers. Iii. Electronic Properties of Polypyrrole. Aust. J. Chem. 1963, 16, 1090-1103.

(7) Vernitskaya, T. y. V.; Efimov, O. N. Polypyrrole: A Conducting Polymer; Its Synthesis , Properties and Applications. Russ. Chem. Rev. 1997, 66, 443-457.

(8) Green, R. A.; Lovell, N. H.; Wallace, G. G.; Poole-Warren, L. A. Conducting Polymers for Neural Interfaces: Challenges in Developing an Effective Long-Term Implant. Biomaterials 2008, 29, 3393-3399.

(9) Granier, T.; Thomas, E. L.; Gagnon, D. R.; Karasz, F. E.; Lenz, R. W. Structure Investigation of Poly(P-phenylene Vinylene). J. Polym. Sci., Part B: Polym. Phys. 1986, 24, 2793-2804.

(10) Burroughes, J. H.; Bradley, D. D. C.; Brown, A. R.; Marks, R. N.; Mackay, K.; Friend, R. H.; Burns, P. L.; Holmes, A. B. Light-Emitting Diodes Based on Conjugated Polymers. Nature 1990, 347, 539-541.

(11) Shacklette, L. W.; Elsenbaumer, R. L.; Chance, R. R.; Eckhardt, H.; Frommer, J. E.; Baughman, R. H. Conducting Complexes of Polyphenylene Sulfides. J. Chem. Phys. 1981, 75, 1919-1927.

(12) Parker, D.; Bussink, J.; van de Grampel, H. T.; Wheatley, G. W.; Dorf, E. -U.; Ostlinning, E.; Reinking, K.; Schubert, F.; Junger, O.; Wagener, R. Polymers, High-Temperature. Ullmann s Encyclopedia of Industrial Chemistry, 2012.

(13) De Surville, R.; Jozefowicz, M.; Yu, L. T.; Pepichon, J.; Buvet, R. Electrochemical Chains Using Protolytic Organic Semiconductors. Electrochim. Acta 1968, 13, 1451-1458.

(14) Yoshikawa, H.; Hino, T.; Kuramoto, N. Effect of Temperature and Moisture on Electrical Conductivity in Polyaniline/Polyurethane (PANI/PU) Blends. Synth. Met. 2006, 156, 1187-1193.

(15) Bagheri, H.; Ayazi, Z.; Naderi, M. Conductive Polymer-Based Microextraction Methods: A Review. Anal. Chim. Acta 2013, 767, 113.

(16) Nezakati, T.; Seifalian, A.; Tan, A.; Seifalian, A. M. Conductive Polymers: Opportunities and Challenges in Biomedical Applications. Chem. Rev. 2018, 118, 6766-6843.

(17) Dubey, N.; Kushwaha, C. S.; Shukla, S. K. A Review on Electrically Conducting Polymer Bionanocomposites for Biomedical and Other Applications. Int. J. Polym. Mater. Polym. Biomater. 2020, 69, 709-727.

(18) Ju, S. A.; Kim, K.; Kim, J.-H.; Lee, S.-S. Graphene-Wrapped Hybrid Spheres of Electrical Conductivity. ACS Appl. Mater. Interfaces 2011, 3, 2904-2911.

(19) Qi, X.-Y.; Yan, D.; Jiang, Z.; Cao, Y.-K.; Yu, Z.-Z.; Yavari, F.; Koratkar, N. Enhanced Electrical Conductivity in Polystyrene Nanocomposites at Ultra-Low Graphene Content. ACS Appl. Mater. Interfaces 2011, 3, 3130-3133.

(20) Yuan, J.-K.; Yao, S.-H.; Sylvestre, A.; Bai, J. Biphasic Polymer Blends Containing Carbon Nanotubes: Heterogeneous Nanotube Distribution and Its Influence on the Dielectric Properties. J. Phys. Chem. C 2012, 116, 2051-2058.

(21) Maiti, S.; Suin, S.; Shrivastava, N. K.; Khatua, B. B. Low Percolation Threshold in Polycarbonate/Multiwalled Carbon Nanotubes Nanocomposites through Melt Blending with Poly(Butylene Terephthalate). J. Appl. Polym. Sci. 2013, 130, 543-553.

(22) Chen, Y.-M.; Ting, J.-M. Ultra High Thermal Conductivity Polymer Composites. Carbon 2002, 40, 359-362.

(23) Ryu, S. H.; Kim, S.; Kim, H.; Kang, S.-O.; Choa, Y.-H. Highly Conductive Polymer Composites Incorporated with Electrochemically Exfoliated Graphene Fillers. RSC Adv. 2015, 5, 36456-36460.

(24) Li, L.; Shi, H.; Liu, Z.; Mi, L.; Zheng, G.; Liu, C.; Dai, K.; Shen, C. Anisotropic Conductive Polymer Composites Based on High Density Polyethylene/Carbon Nanotube/Polyoxyethylene Mixtures for Microcircuits Interconnection and Organic Vapor Sensor. ACS Appl. Nano Mater. 2019, 2, 3636-3647.

(25) Yang, C. Y.; Heeger, A. J. Morphology of Composites of Semiconducting Polymers Mixed with C60. Synth. Met. 1996, 83, 8588.

(26) Shan, X.; Mao, P.; Li, H.; Geske, T.; Bahadur, D.; Xin, Y.; Ramakrishnan, S.; Yu, Z. 3D-Printed Photoactive Semiconducting Nanowire-Polymer Composites for Light Sensors. ACS Appl. Nano Mater. 2020, 3, 969-976.

(27) Okutani, C.; Yokota, T.; Matsukawa, R.; Someya, T. Suppressing the Negative Temperature Coefficient Effect of Resistance in Polymer Composites with Positive Temperature Coefficients of Resistance by Coating with Parylene. J. Mater. Chem. C 2020, 8, 7304-7308.

(28) Zeng, Y.; Lu, G.; Wang, H.; Du, J.; Ying, Z.; Liu, C. Positive Temperature Coefficient Thermistors Based on Carbon Nanotube/ Polymer Composites. Sci. Rep. 2014, 4, 6684.

(29) Han, Z.; Fina, A. Thermal Conductivity of Carbon Nanotubes and Their Polymer Nanocomposites: A Review. Prog. Polym. Sci. 2011, 36, 914-944.

(30) Gu, J.; Zhang, Q.; Dang, J.; Xie, C. Thermal Conductivity Epoxy Resin Composites Filled with Boron Nitride. Polym. Adv. Technol 2012, 23, 1025-1028.

(31) Pang, H.; Xu, L.; Yan, D.-X.; Li, Z.-M. Conductive Polymer Composites with Segregated Structures. Prog. Polym. Sci. 2014, 39, 1908-1933.

(32) Gu, J.; Guo, Y.; Lv, Z.; Geng, W.; Zhang, Q. Highly Thermally Conductive POSS-g-SiCp/UHMWPE Composites with Excellent Dielectric Properties and Thermal Stabilities. Composites, Part A 2015, 78, 95-101.

(33) Sumita, M.; Sakata, K.; Asai, S.; Miyasaka, K.; Nakagawa, H. Dispersion of Fillers and the Electrical Conductivity of Polymer Blends Filled with Carbon Black. Polym. Bull. 1991, 25, 265-271.

(34) Potschke, P.; Bhattacharyya, A. R.; Janke, A. Morphology and Electrical Resistivity of Melt Mixed Blends of Polyethylene and Carbon Nanotube Filled Polycarbonate. Polymer 2003, 44, 80618069.

(35) Li, Y.; Shimizu, H. Conductive PVDF/PA6/CNTs Nanocomposites Fabricated by Dual Formation of Cocontinuous and Nanodispersion Structures. Macromolecules 2008, 41, 5339-5344.

(36) Buys, Y. F.; Aoyama, T.; Akasaka, S.; Asai, S.; Sumita, M. Utilization of Polymer Degradation to Modify Electrical Properties of Poly(l-Lactide)/Poly(Methyl Methacrylate)/Carbon Filler Composites. Compos. Sci. Technol 2010, 70, 200-205.

(37) Vleminckx, G.; Bose, S.; Leys, J.; Vermant, J.; Wubbenhorst, M.; Abdala, A. A.; Macosko, C.; Moldenaers, P. Effect of Thermally Reduced Graphene Sheets on the Phase Behavior, Morphology, and Electrical Conductivity in Poly[(Amethyl Styrene)-Co-(Acryloni-trile)/Poly(Methyl-Methacrylate) Blends. ACS Appl. Mater. Interfaces 2011, 3, 3172-3180.

(38) Mao, C.; Zhu, Y.; Jiang, W. Design of Electrical Conductive Composites: Tuning the Morphology to Improve the Electrical Properties of Graphene Filled Immiscible Polymer Blends. ACS Appl. Mater. Interfaces 2012, 4, 5281-5286.

(39) Chen, J.; Shen, Y.; Yang, J.-h.; Zhang, N.; Huang, T.; Wang, Y.; Zhou, Z.-w. Trapping Carbon Nanotubes at the Interface of a Polymer Blend through Adding Graphene Oxide: A Facile Strategy to Reduce Electrical Resistivity. J. Mater. Chem. C 2013, 1, 7808-7811.

(40) Huang, J.; Zhu, Y.; Xu, L.; Chen, J.; Jiang, W.; Nie, X. Massive Enhancement in the Thermal Conductivity of Polymer Composites by Trapping Graphene at the Interface of a Polymer Blend. Compos. Sci. Technol. 2016, 129, 160-165.

(41) Bai, L.; He, S.; Fruehwirth, J. W.; Stein, A.; Macosko, C. W.; Cheng, X. Localizing Graphene at the Interface of Cocontinuous Polymer Blends: Morphology, Rheology, and Conductivity of Cocontinuous Conductive Polymer Composites. J. Rheol 2017, 61, 575-587.

(42) Bai, L.; Sharma, R.; Cheng, X.; Macosko, C. W. Kinetic Control of Graphene Localization in Co-Continuous Polymer Blends via Melt Compounding. Langmuir 2018, 34, 1073-1083.

(43) Kultravut, K.; Kuboyama, K.; Ougizawa, T. Effect of Blending Procedure on Tensile and Degradation Properties of Toughened Biodegradable Poly(Lactic Acid) Blend with Poly(Trimethylene Terephthalate) and Reactive Compatibilizer. Macromol Mater. Eng. 2019, 304, 1900323.

(44) Kultravut, K.; Kuboyama, K.; Ougizawa, T. Annealing Effect on Tensile Property and Hydrolytic Degradation of Biodegradable Poly(Lactic Acid) Reactive Blend with Poly(Trimethylene Tereph-thalate) by Two-Step Blending Procedure. Polym. Degrad. Stab. 2020, 179, 109228.

(45) Stankovich, S.; Dikin, D. A.; Dommett, G. H. B.; Kohlhaas, K. M.; Zimney, E. J.; Stach, E. A.; Piner, R. D.; Nguyen, S. T.; Ruoff, R. S. Graphene-Based Composite Materials. Nature 2006, 442, 282-286.

(46) Kim, H.; Abdala, A. A.; Macosko, C. W. Graphene/Polymer Nanocomposites. Macromolecules 2010, 43, 6515-6530.

(47) Potts, J. R.; Murali, S.; Zhu, Y.; Zhao, X.; Ruoff, R. S. Microwave-Exfoliated Graphite Oxide/Polycarbonate Composites. Macromolecules 2011, 44, 6488-6495.

(48) Shahil, K. M. F.; Balandin, A. A. Graphene-Multilayer Graphene Nanocomposites as Highly Efficient Thermal Interface Materials. Nano Lett. 2012, 12, 861-867.

(49) Song, S. H.; Park, K. H.; Kim, B. H.; Choi, Y. W.; Jun, G. H.; Lee, D. J.; Kong, B.-S.; Paik, K.-W.; Jeon, S. Enhanced Thermal Conductivity of Epoxy-Graphene Composites by Using Non-Oxidized Graphene Flakes with Non-Covalent Functionalization. Adv. Mater. 2013, 25, 732-737.

(50) Mrlík, M.; Ilcíková, M.; Plachy, T.; Pavlínek, V.; Spitalsky, Z.; Mosnácek, J. Graphene Oxide Reduction during Surface-Initiated Atom Transfer Radical Polymerization of Glycidyl Methacrylate: Controlling Electro-Responsive Properties. Chem. Eng. J. 2016, 283, 717-720.

(51) Mrlík, M.; Ilcíková, M.; Plachy, T.; Moučka, R.; Pavlínek, V.; Mosnácek, J. Tunable Electrorheological Performance of Silicone Oil Suspensions Based on Controllably Reduced Graphene Oxide by Surface

Initiated Atom Transfer Radical Polymerization of Poly-(Glycidyl Methacrylate). J. Ind. Eng. Chem. 2018, 57, 104-112.

(52) Brodie, B. C. On the Atomic Weight of Graphite. Philos. Trans. R. Soc. London 1859, 149, 249-259.

(53) Morikawa, J.; Hashimoto, T. Thermal Diffusivity of Aromatic Polyimide Thin Films by Temperature Wave Analysis. J. Appl. Phys. 2009, 105, 113506.

(54) Hwang, T. Y.; Yoo, Y.; Lee, J. W. Electrical Conductivity, Phase Behavior, and Rheology of Polypropylene/Polystyrene Blends with Multi-Walled Carbon Nanotube. Rheol. Acta 2012, 51, 623-636.

(55) Meador, M. A. B.; Hardy-Green, D.; Auping, J. V.; Gaier, J. R.; Ferrara, L. A.; Papadopoulos, D. S.; Smith, J. W.; Keller, D. J. Optimization of Electrically Conductive Films: Poly(3-Methylthio-phene) or Polypyrrole in Kapton. J. Appl. Polym. Sci. 1997, 63, 821834.

(56) Morishita, T.; Matsushita, M.; Katagiri, Y.; Fukumori, K. A Novel Morphological Model for Carbon Nanotube/Polymer Composites Having High Thermal Conductivity and Electrical Insulation. J. Mater. Chem. 2011, 21, 5610-5614.

(57) Shi, Y.-y.; Yang, J.-h.; Huang, T.; Zhang, N.; Chen, C.; Wang, Y. Selective localization of carbon nanotubes at the interface of Poly(L-lactide)/Ethylene-co-vinyl Acetate resulting in lowered electrical resistivity. Composites, Part B 2013, 55, 463-469.

(58) Mun, S. C.; Kim, M. J.; Cobos, M.; Gu, L.; Macosko, C. W. Strategies for interfacial localization of graphene/polyethylene-based cocontinuous blends for electrical percolation. AIChE J. 2019, 65, No. e16579.

(59) Hosseinpour, A.; Nasseri, R.; Ghiassinejad, S.; Mehranpour, M.; Katbab, A. A.; Nazockdast, H. Improving the Electrical Conductivity of Ethylene 1-Octene Copolymer/Cyclic Olefin Copolymer Immiscible Blends by Interfacial Localization of MWCNTs. Polym. Eng. Sci. 2019, 59, 447-456.

(60) Tu, C.; Nagata, K.; Yan, S. Influence of melt-mixing processing sequence on electrical conductivity of polyethylene/polypropylene blends filled with graphene. Polym. Bull. 2017, 74, 1237-1252.

(61) Zhang, Z.; Cao, M.; Chen, P.; Yang, B.; Wu, B.; Miao, J.; Xia, R.; Qian, J. Improvement of the thermal/electrical conductivity of PA6/PVDF blends via selective MWCNTs-NH2 distribution at the interface. Mater. Des. 2019, 177, 107835.

(62) Zhang, X.; Maira, B.; Hashimoto, Y.; Wada, T.; Chammingkwan, P.; Thakur, A.; Taniike, T. Selective localization of aluminum oxide at interface and its effect on thermal conductivity in polypropylene/polyolefin elastomer blends. Composites, Part B 2019, 162, 662-670.

(63) Salehiyan, R.; Ray, S. S. Tuning the Conductivity of Nanocomposites through Nanoparticle Migration and Interface Crossing in Immiscible Polymer Blends: A Review on Fundamental Understanding. Macromol. Mater. Eng. 2019, 304, 1800431.